

High-Selectivity On-Chip Optical Bandpass Filter With Sub-100-MHz Flat-Top and Under-2 Shape Factor

Caterina Taddei^{ID}, Leimeng Zhuang^{ID}, Chris G. H. Roeloffzen^{ID}, Marcel Hoekman^{ID}, and Klaus-J. Boller

Abstract—We demonstrate a fully tunable microwave photonic bandpass filter fabricated with Si₃N₄/SiO₂ waveguides on a chip. The filter is based on coupled resonator optical waveguide architecture comprising a chain of eight coupled ring resonators, each with an optical roundtrip length of 21 cm (free spectral range of 1.4 GHz), with an adjustable resonance frequency, and with adjustable power coupling. The passband shows a 3-dB bandwidth of 72 MHz with at least 51-dB out-of-band rejection and features simultaneously a flat-top, a shape factor of 1.9, and a group delay variation smaller than 2 ns.

Index Terms—Integrated optics, microwave photonic filter, MWP filter, CROW, optical waveguide filter, resonator filter.

I. INTRODUCTION

MICROWAVE photonics (MWP) is a rapidly emerging field that can overcome fundamental limitations of electronics by processing microwave (RF) information in the optical domain [1]–[3]. Main advantages are an approximately thousand-fold increased bandwidth and a strongly reduced energy consumption. Specifically, integrating MWP functions on optical chips (integrated microwave photonics, IMWP) yields superior immunity to external perturbations and a significantly reduced size and weight. Next to tunable true time delay lines, phase shifters or beam-forming networks, a most important functionality is spectral filtering.

An example where such functionalities would form the key towards advanced performance are links within

Manuscript received November 20, 2018; revised January 15, 2019; accepted February 2, 2019. Date of publication February 6, 2019; date of current version March 12, 2019. This work was supported in part by the Rijksdienst voor Onderzoek Nederland through the IOP Photonics Devices Program under the Promis2Day Project and in part by the Netherlands Space Office through the Prequalification for European Space Agency Programs under Project ORPHEUS PEP12032. (Corresponding author: Caterina Taddei.)

C. Taddei is with the Laser Physics and Nonlinear Optics Group, MESA+ Research Institute for Nanotechnology, 7500 Enschede, The Netherlands, and also with Lionix BV, 7500 Enschede, The Netherlands (e-mail: c.taddei@lionix-int.com).

L. Zhuang is with the Electro-Photonics Laboratory, Department of Electrical and Computer Systems Engineering, Monash University at Clayton Campus, Melbourne, VIC 3800, Australia, on leave to IMEC, Kissimmee, FL 34744 USA (e-mail: leimeng.zhuang@ieee.org).

C. G. H. Roeloffzen and M. Hoekman are with Lionix BV, 7500 Enschede, The Netherlands.

K.-J. Boller is with the Laser Physics and Nonlinear Optics Group, MESA+ Research Institute for Nanotechnology, 7500 Enschede, The Netherlands.

Color versions of one or more of the figures in this letter are available online at <http://ieeexplore.ieee.org>.

Digital Object Identifier 10.1109/LPT.2019.2897859

swarms of smart satellites that use on-board processing with flexible re-configurability. Realizing these functions in the RF domain is problematic due to high energy consumption, large size and weight, sensitivity to electromagnetic interference, and also due to lack of flexibility, which is due to the need of handling predetermined data formats. Having appropriate optically integrated filters available would enable Input Multiplexers (IMUX) that accomplish partitioning of the satellite bandwidth into narrow sub-bands (channelization).

In multi-beam satellites, IMUX filters could also be integrated with routing networks and other signal processing functionalities. Specifically required is a filter bandwidth of 36 or 72 MHz and a flat in-band response (<3 dB) with a group delay variation smaller than 2 ns and low insertion loss (<20 dB). Another central requirement is a larger-than-40-dB out-of-band rejection and a high steepness of the transmission function at the filter edges. This is quantitatively described with a small filter Shape Factor (SF), which is defined as the ratio of the 40-dB bandwidth and the 6-dB bandwidth. Desired are values in the order of SF ≈ 2, which is about 30-times steeper than a Lorentzian filter (SF = 58).

However, integrated optical filters that can meet such highly challenging spectral and re-configurational requirements have not been demonstrated so far. The reason is that the required filter bandwidth is extremely narrow as compared to the optical carrier. For instance, a filter bandwidth of 72 MHz at a frequency of 200 THz (1.5 μm wavelength) corresponds to a quality (Q) factors of about three million, which is equivalent to on-chip propagation along huge optical path lengths near ten meters with low loss. A second challenge is that the shape of the transmission spectrum has to be configurable, in order to provide flat and low-dispersion passbands that can be tuned to any desired center frequency.

Here we demonstrate the first integrated MWP filter suitable for operation on board of a satellite – with a flat-top passband of 72 MHz width, a steepness given by SF = 1.9, and an out-of-band rejection larger than 40 dB with less than 2 ns group delay variation. The filter is fully reconfigurable in shape and center frequency. Passband flattening is obtained by forming a so-called Coupled Resonator Optical Waveguide (CROW) [4], [5] with eight ring resonators, each having 21 cm optical length, with an adjustable resonance frequency and adjustable power coupling. The key to such performance is making use of an advanced dielec-

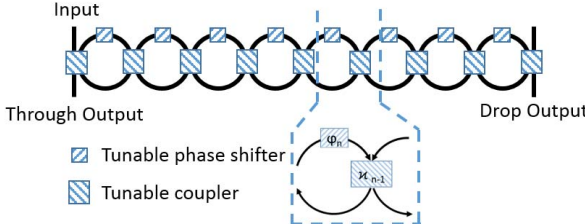


Fig. 1. Functional scheme of the waveguide structure.

tric waveguide platform which offers an ideal combination of high index contrast, ultra-low propagation loss and high maturity for reliable fabrication of complex and reconfigurable circuitry [6], [7]. We note that MWP filters have been demonstrated by others as well, such as with cascaded silicon micro-ring resonators [8], stimulated Brillouin Scattering [9], [10], fiber Bragg gratings [11] and Mach-Zehnder interferometers [12]. These solutions are, however, either relying on bulk components less suitable for application in satellites, require additional pump lasers, or cannot match the spectral requirements in terms of narrow bandwidth.

II. INTEGRATED CIRCUIT DESIGN

The functional scheme of the fabricated filter is given in Fig. 1, where φ_n denotes an adjustable phase shift in the n^{th} ring and where φ_n is the power coupling coefficient between the $n-1^{\text{st}}$ ring and the n^{th} ring.

The optical transmission properties of the circuit was modelled via the Z-transform method [13]. This yields the complex-valued field transfer function *vs.* light frequency within a free spectral range (FSR) mapped onto the 2π -circumference of the unit circle in the complex z-plane. The transfer function from the Input to the Drop Output, and to the Through Output is obtained, respectively, as

$$H_{DRP} = \frac{(-j)^{N+1} \sqrt{\sigma_N e^{j\varphi_{tot}} \gamma^N} z^{-N}}{A_N(z)} \quad (1)$$

$$H_{THR} = \frac{B_N(z)}{A_N(z)}. \quad (2)$$

In Eq.1, N is the number of coupled resonators, $\sigma_N = \prod_{n=0}^N \chi_n$ is the product of the power coupling coefficients, $\varphi_{tot} = \sum_{n=1}^N \varphi_n$ is the total phase shift imposed by the resonators, and $\gamma \leq 1$ is the amplitude transmission coefficient per roundtrip through a ring, which is determined by the waveguide loss. $A_N(z)$ and $B_N(z)$ are two N^{th} order polynomials in z^{-1} , with their coefficients depending on the values of χ_n and φ_n [13]. H_{DRP} has poles in the complex plane, while H_{THR} has both poles and zeros, being the ratio of two polynomials.

In order to impose a maximally flat spectral shape with high steepness and rejection, we have calculated the settings of the coupling coefficients that provide a maximally flat peak in $H_{DRP}(z)$. Maximum flatness is obtained with a so-called Butterworth filter (here of 8th order). The according coefficients and phases were derived as displayed in Table 1, using the modified Levinson algorithm [14]. Deviation of any phase from zero leads to asymmetric spectra. We note that the shown values provide the optimum transmission functions for the

TABLE I
OPTIMUM CIRCUIT PARAMETERS FOR A MAXIMALLY FLATTENED (BUTTERWORTH) MICROWAVE PHOTONIC FILTER REALIZED AS AN 8th-ORDER CROW CALCULATED VIA [14]

Parameter	Theoretical value Derived via [14]
χ_0, χ_8	0.343
χ_1, χ_7	0.025
χ_2, χ_6	0.011
χ_3, χ_5	0.009
χ_4	0.0085
φ_1 to φ_8	0°

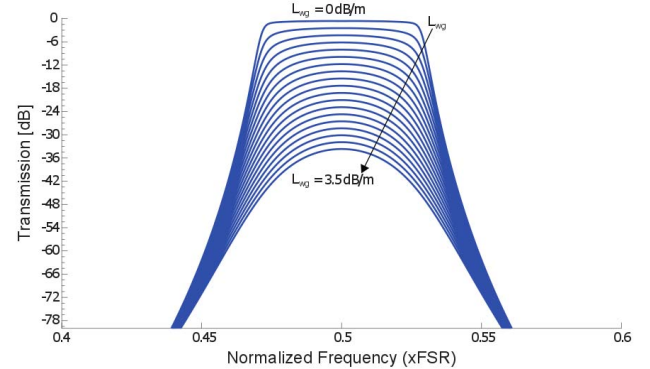


Fig. 2. Power transmission spectrum for linearly increasing waveguide loss.

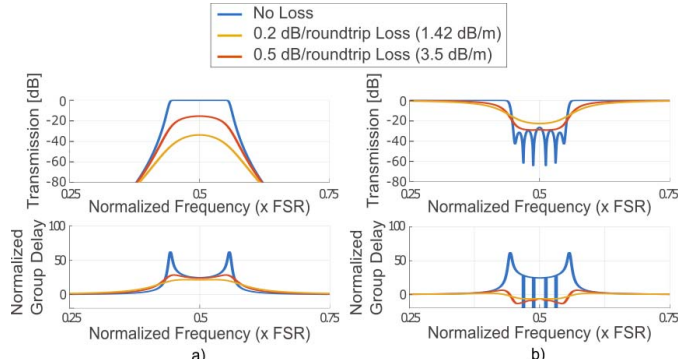


Fig. 3. Calculated power transmission and normalized group delay for (a) the drop output and (b) the through output.

assumption of zero loss ($\gamma = 1$). For $\gamma < 1$, different values are expected that depend on the assumed waveguide loss. The accordingly calculated power transmission to the Drop output *vs.* frequency in units of the free spectral range is shown in Fig. 2, for various different values of the waveguide loss parameter. It can be seen the spectral shape deviates progressively from the desired flat shape (small SF) towards a rounded shape (higher SF) if the waveguide loss parameter is increased, even if the assumed loss is rather small (< 3.5 dB/m).

This limitation does not only affect the passband profile but also the group delay dispersion, as is shown in III: as the loss increases, the 3-dB bandwidth becomes smaller through progressing curvature, whereas the group delay is least dispersive at some intermediate loss value.

Similarly, the transmission band in the Through output becomes rounded whereas intermediate losses yield the least dispersive shape. From the lowering of the peak transmission

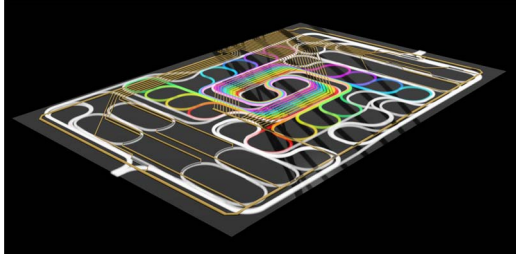


Fig. 4. Layout of the fabricated (55mm x 35 mm) chip where the individual eight resonators (displayed in separate colors) are wound into each other.

in the Drop output one can see that the insertion loss increases with the waveguide loss parameter.

We note that all of these calculations and considerations still involve extremely low levels of waveguide loss, namely below 0.035 dB/cm (< 3.5 dB/m). This underlines the central importance of selecting a waveguide platform that can offer such low loss and still allows to implement complex waveguide circuits on a small, chip-sized area.

III. FABRICATION AND DEMONSTRATION

We have fabricated the circuit shown in Fig. 1 using Si_3N_4 waveguides in a SiO_2 cladding [15] to obtain low propagation loss [16] as well as a high index contrast for reducing bending loss [6]. The power coupling coefficients and phase shifters can be thermo-electrically tuned with resistive thin film heaters. The fabricated chip has been designed for a FSR of 1.4 GHz. A graphical impression of the fabricated chip is shown in Fig. 4.

The chip is bound to a printed circuit board connected to a flat cable, and each heater is addressed by a computer via USB through a custom developed control board. The optical inputs and outputs are connected to fiber arrays. Using a straight test waveguide on the same chip, we measured a fiber-to-chip coupling loss of about 3 dB/facet.

For the experimental characterization of the MWP filter, a single-frequency laser (EM4-253-80-057, spectral bandwidth 1 MHz) is used as optical carrier and is amplitude-modulated by a 10-MHz signal from an RF Vector Network Analyzer (VNA, Agilent NA5230A PNA-L), before sending the light into the CROW filter. To measure the frequency response across one or more FSRs, the laser wavelength is tuned via the laser drive current. The output from the filter is detected by a photodiode (Discovery Semiconductor DSC-R401 HG, bandwidth 20 GHz) and sent to the VNA for measuring power and phase of the transmitted signals *vs.* light frequency.

The transmission spectra were manually optimized to a best compromise of narrowest bandwidth, highest flatness and lowest group delay dispersion. The accordingly required settings for the heater elements were found with separate experimental calibration of the circuit parameters of each ring resonator, before setting the parameters to the theoretically expected optimum values (Table 1). The adjustment of the phases was done by minimizing any spectral asymmetry in the transmission spectrum. Improvements in steepness, flatness and bandwidth narrowing were performed manually, although ultimately a computer control can be applied as well.

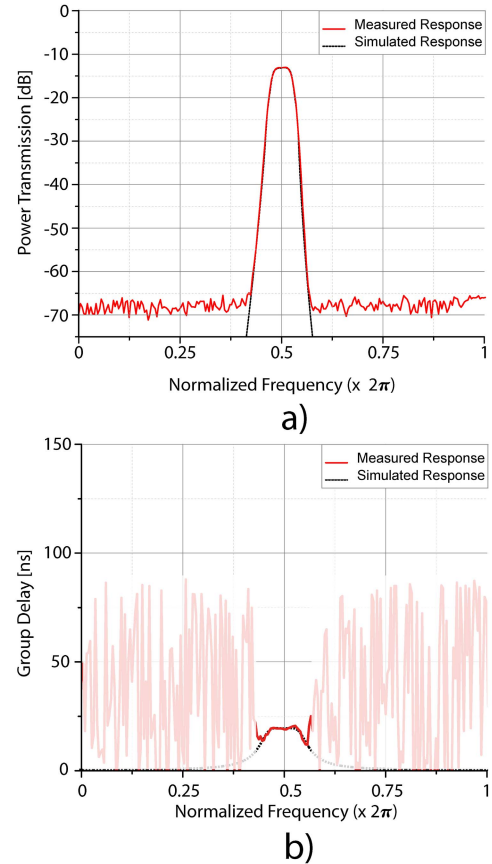


Fig. 5. Measured and simulated a) RF transmission response and b) group delay of the drop output of the fabricated CROW filter.

The measured power and group delay spectra after optimization are plotted in Fig. 5.

The measured passband bandwidth of 72 MHz, which is, to the best of our knowledge, the narrowest-ever bandwidth obtained for an integrated MWP filter using only passive components. The measured maximum group delay variation in the passband is approximately 2 ns. The measured filter transmission and delay are in excellent agreement with the theoretical model when using model parameters close to the ideal values. The measured shape factor of the filter, $SF = 1.93$, is rather close to the ultimate lossless limit ($SF = 1.34$). The out-of-band rejection, particularly interesting when the filter is employed as IMUX to reject adjacent channels, is at least 51 dB (limited by the experimental noise floor of the equipment). The overall insertion loss of the filter is 13 dB. From this value and the parameters in the theoretical curves in Fig. 2, we estimate that waveguide loss is as low as 0.014 dB/cm (1.4 dB/m).

To demonstrate reconfigurability, we have tuned the transmission to an adjacent spectral interval by a larger distance that is about half of the FSR, in this case about 0.7 GHz. It can be seen in Fig. 6 that the shape and out-of-band rejection of the filter are reproduced with high fidelity. This feature allows an active change of the parameters in order to have the filter centered at any desired frequency within the FSR. For further characterization, the transfer function to the Through output

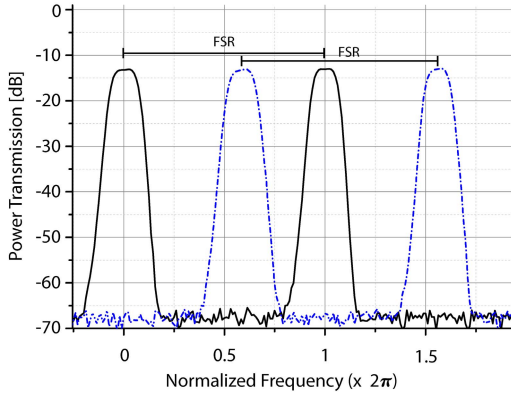


Fig. 6. Power transmission response measured tuning the filter at two different center frequencies.

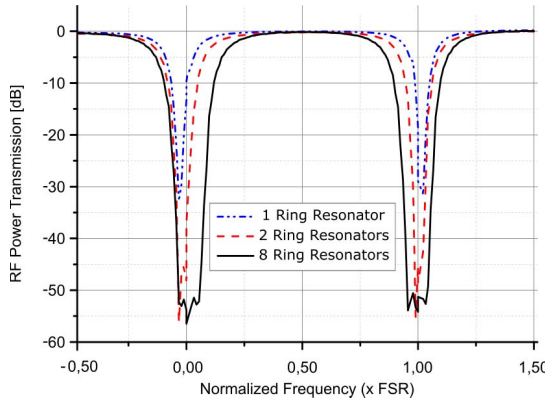


Fig. 7. Power transmission response of the through output port for different optical parameters setting.

was inspected as well. An example is shown in IV, where the power transmission is displayed for the following three different settings of the optical couplers. The dotted blue curve is measured when setting the coupler χ_1 , between the first ring and the second ring, to zero, assuming a lossy case. All the other power coupling coefficients are set to 1. In this case one obtains the transmission function of a simple (1st-order) notch filter that can be tuned with the input coupler (χ_0) between the bus waveguide and the first ring. The measured FWHM for the notch filter is 14 MHz, which corresponds to a finesse of about 100, confirming the waveguide loss value named above. Analogously, manipulating the coupler to the second resonator generates a wider (2nd-order filter) with similar slope at the filter edges, progressing towards an 8th-order filter.

IV. CONCLUSION

We have demonstrated an integrated optical passband MWP filter based on a CROW structure comprising $N = 8$ resonators. The filter has been fabricated using an ultra-low loss waveguide platform based on a Si₃N₄ core in a SiO₂ cladding.

The filter shows a record narrow, passband flattened bandwidth of 72 MHz (filter shape factor 1.93) and an out-of-band rejection of at least 51 dB. These values indicate a very low waveguide loss of around 0.014 dB/cm and large effective optical length of about five meters on a chip. The filter is fully tunable and reconfigurable in shape and center frequency. In combination with the Through port output response of the same CROW filter it appears feasible to integrate multiple DMUX and MUX functionalities. The compact and rugged format and high energy efficiency of such microwave photonic processing devices appear suitable even for demanding applications, such as in smart satellite systems.

REFERENCES

- [1] J. Capmany, B. Ortega, and D. Pastor, "A tutorial on microwave photonic filters," *J. Lightw. Technol.*, vol. 24, pp. 201–229, Jan. 2006.
- [2] S. Iezekiel, M. Burla, J. Klamkin, D. Marpaung, and J. Capmany, "RF engineering meets optoelectronics: Progress in integrated microwave photonics," *IEEE Microw. Mag.*, vol. 16, no. 8, pp. 28–45, Sep. 2015.
- [3] J. Capmany and P. Muñoz, "Integrated microwave photonics for radio access networks," *J. Lightw. Technol.*, vol. 32, pp. 2849–2861, Aug. 15, 2014.
- [4] F. Morichetti, C. Ferrari, A. Canciamilla, and A. Melloni, "The first decade of coupled resonator optical waveguides: Bringing slow light to applications," *Laser Photon. Rev.*, vol. 6, no. 1, pp. 74–96, 2012.
- [5] J. Capmany, P. Muñoz, J. D. Domenech, and M. A. Muriel, "Apodized coupled resonator waveguides," *Opt. Express*, vol. 15, no. 16, pp. 10196–10206, Aug. 2007.
- [6] K. Wörhoff, R. G. Heideman, A. Leinse, and M. Hoeckman, "TriPleX: A versatile dielectric photonic platform," *Adv. Opt. Technol.*, vol. 4, no. 2, pp. 189–207, 2015.
- [7] C. G. H. Roeloffzen *et al.*, "Silicon nitride microwave photonic circuits," *Opt. Exp.*, vol. 21, no. 19, pp. 22937–22961, Jun. 2013.
- [8] L. Liu, M. He, and J. Dong, "Compact continuously tunable microwave photonic filters based on cascaded silicon microring resonators," *Opt. Commun.*, vol. 363, pp. 128–133, Mar. 2016.
- [9] X. Zou, W. Li, W. Pan, L. Yan, and J. Yao, "Photonic-assisted microwave channelizer with improved channel characteristics based on spectrum-controlled stimulated Brillouin scattering," *IEEE Trans. Microw. Theory Techn.*, vol. 61, no. 9, pp. 3470–3478, Sep. 2013.
- [10] A. Choudhary *et al.*, "Tailoring of the Brillouin gain for on-chip widely tunable and reconfigurable broadband microwave photonic filters," *Opt. Lett.*, vol. 41, no. 3, pp. 436–439, Feb. 2016.
- [11] L. Gao, X. Chen, and J. Yao, "Tunable Microwave Photonic Filter With a Narrow and Flat-Top Passband," *IEEE Microw. Wireless Compon. Lett.*, vol. 23, no. 7, pp. 362–364, Jul. 2013.
- [12] J. Mora *et al.*, "Photonic microwave tunable single-bandpass filter based on a Mach-Zehnder interferometer," *J. Lightw. Technol.*, vol. 24, no. 7, pp. 2500–2509, Jul. 2006.
- [13] B. Moslehi, J. W. Goodman, M. Tur, and H. J. Shaw, "Fiber-optic lattice signal processing," *Proc. IEEE*, vol. 72, no. 7, pp. 909–930, Jul. 1984.
- [14] C. K. Madsen and J. H. Zhao, *Optical Filter Design and Analysis: A Signal Processing Approach*. Hoboken, NJ, USA: Wiley, 1999, pp. 246–250.
- [15] C. G. H. Roeloffzen *et al.*, "Low-Loss Si₃N₄ TriPleX optical waveguides: Technology and applications overview," *IEEE J. Sel. Topics Quantum Electron.*, vol. 24, no. 4, Jul./Aug. 2018, Art. no. 4400321.
- [16] J. Bauters *et al.*, "Planar waveguides with less than 0.1 dB/m propagation loss fabricated with wafer bonding," *Opt. Exp.*, vol. 19, no. 24, pp. 24090–24101, 2011.